

pubs.acs.org/NanoLett Letter

Morphological Transitions of a Photoswitchable Aramid Amphiphile Nanostructure

Dae-Yoon Kim, ^L Ty Christoff-Tempesta, ^L Guillaume Lamour, Xiaobing Zuo, Ki-Hyun Ryu, and Julia H. Ortony*



Cite This: Nano Lett. 2021, 21, 2912-2918



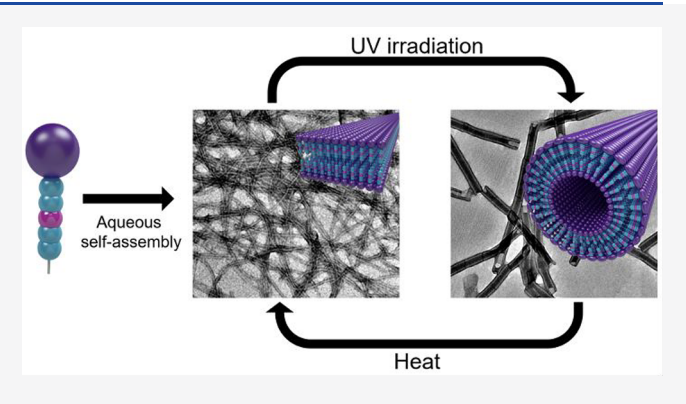
ACCESS

Metrics & More



SI Supporting Information

ABSTRACT: Self-assembly of small amphiphilic molecules in water can lead to nanostructures of varying geometries with pristine internal molecular organization. Here we introduce a photoswitchable aramid amphiphile (AA), designed to exhibit extensive hydrogen bonding and robust mechanical properties upon self-assembly, while containing a vinylnitrile group for photoinduced *cis—trans* isomerization. We demonstrate spontaneous self-assembly of the vinylnitrile-containing AA in water to form nanoribbons. Upon UV irradiation, *trans*-to-*cis* isomerizations occur concomitantly with a morphological transition from nanoribbons to nanotubes. The nanotube structure persists in water for over six months, stabilized by strong and collective intermolecular interactions. We demonstrate that the nanoribbon-



to-nanotube transition is reversible upon heating and that switching between states can be achieved repeatedly. Finally, we use electron microscopy to capture the transition and propose mechanisms for nanoribbon-to-nanotube rearrangement and vice versa. The stability and switchability of photoresponsive AA nanostructures make them viable for a range of future applications.

KEYWORDS: Small-molecule self-assembly, aramid amphiphile, photoisomerization, nanoribbon, nanotube

olecular self-assembly of amphiphilic small molecules in water provides a route to nanostructures with high surface areas and versatile surface chemistries. The dimensions of self-assembled nanostructures are determined by the lengths of their constituent molecules; in turn, amphiphilic molecules assemble to form nanostructures with dimensions on the order of 10 nm along at least one axis and high surface areas. Further, these architectures readily allow for the inclusion of functional molecules by coassembly, facilitating reactions or recognition events at their surfaces. Amphiphilic self-assembly is governed by noncovalent interactions and therefore leads to dynamic and path-dependent morphologies. Such materials have shown great promise as biomaterials, where fast conformational dynamics are an important feature, and also in the area of systems chemistry, which exploits collective behaviors of ensembles of molecules governed by their dynamic nature.

Imparting photoswitching capabilities within self-assembled small-molecule nanostructures is an important target for introducing new functions. Phototriggers have been combined with amphiphilic self-assembly for a variety of purposes: to liberate surface-bound cell signaling moieties from bioactive nanofiber matrices, ¹⁸ to modulate bilayer membrane fluidity, ¹⁹ to disrupt the balance of *cis-trans* equilibria by selectively arresting one isomer into an assembled structure, ²⁰ to

modulate mechanical properties for photolithography and adhesion/lubrication applications, ²¹ and for photoinitiated synthesis of amphiphiles in water. ²² However, photoisomerization in these systems has generally so far only led to relatively short-lived metastable states, with half-lives ranging from seconds to days. ²³ We hypothesize that achieving a morphological transition whose reverse reaction also requires input energy may be accomplished by tuning the intermolecular interaction strengths within the metastable nanostructure

Though less frequently used, the isomerized products of stilbene-derived chromophores are more stable in contrast to those from conventional azobenzene dyes and can be used to enhance the half-life of a metastable nanostructure. Vinylnitrile-based groups—a class of stilbene-derived chromophores—incorporated in a molecular structure can be isomerized by irradiation from the *trans* to *cis* state and spontaneously revert slowly (on the order of minutes to days)

Received: December 28, 2020 Revised: February 24, 2021 Published: March 18, 2021





at room temperature. ^{23,28,29} Thus, programming the design of photoresponsive small molecules can allow us to tune molecular self-assembled nanoarchitectures with desirable dimensions and time-stable morphologies.

Here, we investigate the phototriggered isomerization reaction of amphiphiles after self-assembly into strongly cohesive nanoribbons in water. The chemical structure of the small-molecule constituents is designed to exhibit (1) strong and extensive intermolecular interactions and (2) a photoactive moiety known for a dramatic geometric transition upon a 365 nm UV (UVA) light irradiation. This approach is hypothesized to induce molecular isomerization for reversible morphological transitions, with structural stability in both the *trans* and *cis* morphological states.

A strong and extensive network of intermolecular interactions within the nanostructure is achieved by employing aramid amphiphile (AA) molecules. AAs have previously been show to assemble spontaneously in water to form nanoribbons with thicknesses and widths under 10 nm and lengths greater than tens of microns. Within AA nanoribbons, each molecule is fixed in place by six in-register hydrogen bonds propagating down the length of the nanoribbon and $\pi-\pi$ stacking across its width. This network of strong interactions suppresses molecular exchange and migration within assemblies and produces nanoribbons with robust mechanical properties, rivaling silk. ³⁰

AAs are composed of a hydrophilic headgroup, an aramid structural domain, and a hydrophobic tail (Figure 1a). Here, we design a photoswitchable analogue to the conventional AA molecule which incorporates a vinylnitrile group into the center of the aramid structural domain (Figure 1b). This molecule is designed to similarly form nanoribbons in water but further exhibit a morphological transition upon UVA

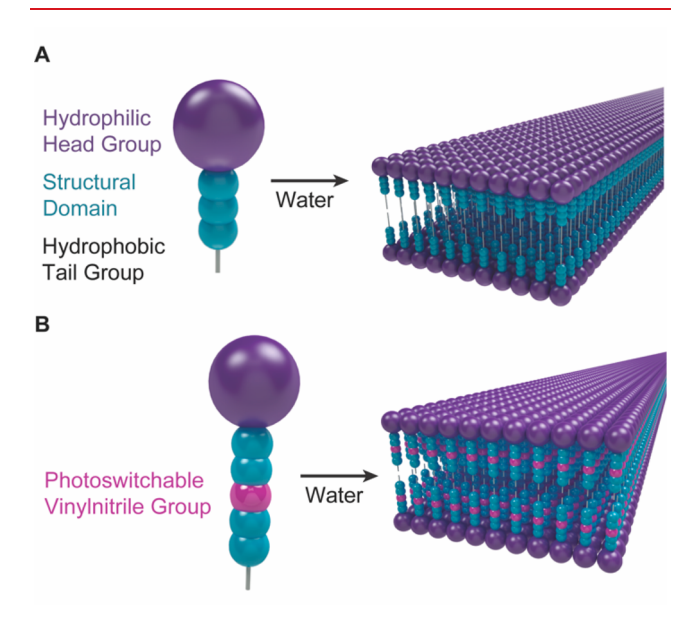


Figure 1. Aramid amphiphiles (AAs) self-assemble in water to form nanoribbons. Their stabilities are bolstered by strong intermolecular hydrogen bonding between adjacent aramid structural domains. (a) Conventional AAs self-assemble in water to form planar nanoribbons with no photo-responsive behavior. (b) Photoresponsive AAs, designed analogously to conventional AAs but with a vinylnitrile moiety in the center of the aramid domain, are designed to assemble into nanoribbons in water with triggerable morphological transitions.

irradiation. The effect of isomerization of adjacent vinylnitrile groups and the strong intermolecular interactions within the nanostructure are hypothesized to dramatically increase the lifetime of the isomerized product. Compound 1 (Figure 2a) is selected as a control for this experiment for its similar chemical structure and equivalent number of hydrogen bonds as compound 2 (Figure 2d).

Compound 1 is an AA that spontaneously self-assembles in water to form high-aspect-ratio nanoribbons (Figure 2b).

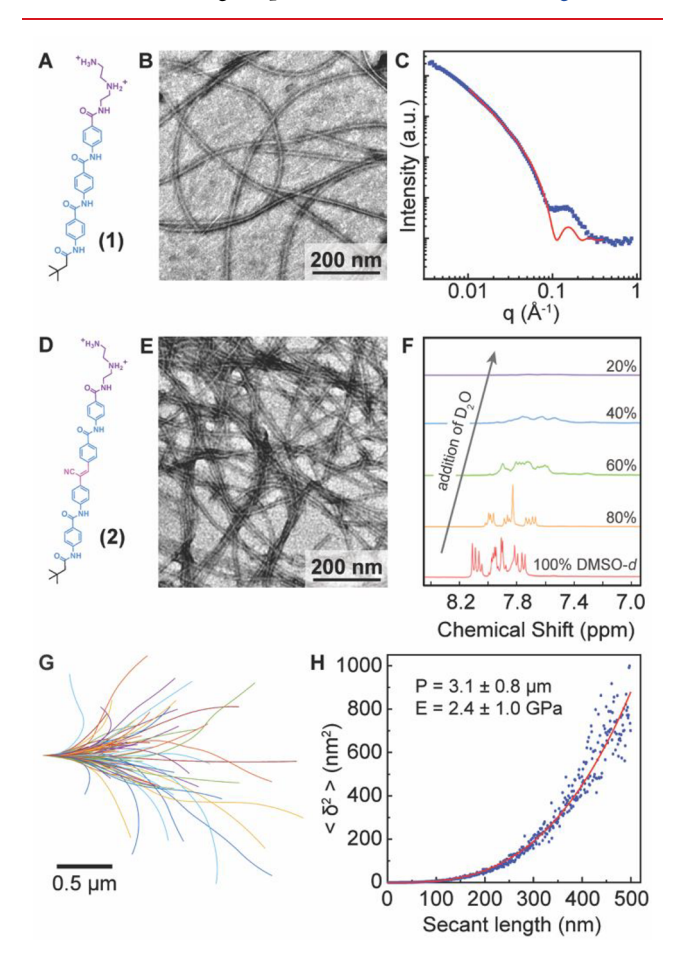


Figure 2. Both conventional and photoswitchable AAs form nanoribbons in water. (a,b) Compound 1 is a conventional AA with a cationic headgroup (purple), aramid structural domain (blue), and short aliphatic tail (black) that spontaneosuly forms nanoribbons with 5.8 nm widths upon assembly in water. (c) Compound 1 nanoribbons are determined to have 3.9 nm thicknesses based on lamellar fitting (red line) to SAXS. (d) Compound 2 incorporates a photoswitchable vinylnitrile moiety (pink) into the aramid amphiphile design. (e) Compound 2 forms nanoribbons mimicking those of compound 1 upon spontaneous assembly in water. (f) The assembly of compound 2 is observed by ¹H NMR of the aromatic molecular region as the ratio of D₂O to DMSO-d increases. Assembly of the amphiphiles in D2O results in an upfield proton shift from magnetic shielding and peak broadening from slowing conformational dynamics. (g) Contours of compound 2 nanoribbons (n = 96) are traced from AFM profiles for statistical topographical analysis. (h) Midpoint deviations (δ) from the contour traces of compound 2 nanoribbons are used to derive a Young's modulus of $E = 2.4 \pm 1.0$ GPa from calculating a persistence length, $P = 3.1 \pm 0.8 \mu m$, by leastsquares fitting of a worm-like chain model for semiflexible polymers (red line) to the data. This stiffness value closely matches that of prototypical AAs.

Compound 1 nanoribbons exhibit strong internal cohesion resulting in suppressed exchange dynamics. The small-angle X-ray scattering (SAXS) profile of 1 at a concentration of 30 mg/mL is fit (Figure 2c, Figure S13) to determine nanoribbon thickness of 3.9 nm. The widths of 1 nanoribbons is approximated from TEM as 5.8 nm. 31

Compound **2** is obtained following similar reactions as previously reported.³⁰ In short, the molecule is built up with alternating carbodiimide-mediated amidation coupling reactions and standard deprotection reactions, and uses the Knoevenagel reaction to obtain the target compound. Detailed synthetic methods are described in Supporting Information Sections S2 and S6. The chemical structures and purities are confirmed by ¹H and ¹³C nuclear magnetic resonance (NMR), matrix-assisted laser desorption and ionization time-of-flight (MALDI-ToF) mass spectrometry, and elemental analysis.

We first seek to understand the self-assembly behavior of compound 2 in water. As previously observed for compound 1, compound 2 spontaneously forms high-aspect-ratio nanoribbons with lengths on the order of microns upon assembly in water (Figure 2e). Hydrogen bonding between amides in the aramid structural domain is likely the main driving force in forming the elongated nanoribbon structure. $\pi-\pi$ stacking assists in holding the hydrogen bonding sheets laterally, and the local dipole moments of the cyanide can further help to induce side-to-side intermolecular coupling.

Molecular interaction resulting from the self-assembly of ${\bf 2}$ in water can be investigated via solvent variation (Figure 2f). Compound ${\bf 2}$ is highly soluble in deuterated dimethyl sulfoxide (DMSO-d), resulting in a monomeric state. This is observed in the 1H NMR spectra of ${\bf 2}$ by well-resolved, sharp peaks, shown for aromatic rings in the structural domain. These proton peaks widen and shift upfield when deuterated water (D₂O) is titrated into the solution. The gradual broadening of these peaks is concomitant with the formation of strong intermolecular interactions and the slowing of conformational dynamics upon self-assembly of ${\bf 2}$ in water. The upfield shift of protons results from the tightening of intermolecular distances with assembly that induces a magnetic shielding effect. No nanoribbons or other nanostructures are observed by TEM when ${\bf 1}$ or ${\bf 2}$ is dissolved in 100% DMSO-d.

Compound 1 nanoribbons were previously shown to exhibit a Young's modulus $E = 1.7 \pm 0.7$ GPa.³⁰ Here, we employ a statistical topographical analysis of nanoribbon contours to determine if incorporating the photoswitchable vinylnitrile moiety impacts the nanoribbons' mechanical properties (SI Section S8). This technique overcomes the lower size bound limitations of direct mechanical measurements, enabling stiffness measurements on nanofilaments with diameters below 10 nm. ^{32,33} The contours of n = 96 compound 2 nanoribbons in water were captured by atomic force microscopy (Figure 2g). Parametric splines were extracted from each contour and used to obtain a nanoribbon persistence length of $P = 3.1 \pm 0.8 \ \mu m$, from which a Young's modulus of $E = 2.4 \pm 1.0$ GPa is calculated (Figure 2h). This stiffness closely matches the previously reported stiffness for compound 1 nanoribbons, 30 likely resulting from similar intermolecular interaction strengths and hydrogen bond densities between the amphiphiles.

Molecular-scale isomerizations of photoresponsive aromatic molecules result in changes in absorbance that can be detected by UV—vis absorption spectroscopy. As expected, we observe no change in absorbance of aqueous solutions of 1 upon 1 h of

irradiation with UVA light (0.1 mg/mL, 1500 mW/cm², Figure S18). In contrast, a 0.1 mg/mL solution of compound 2 dissolved in dimethyl sulfoxide (DMSO) shows a dramatic reduction in peak intensity at $\lambda_{\rm max} = 350$ nm under the same conditions (Figure S19). This spectral change indicates that the vinylnitrile *cis* isomer is increased during irradiation with a corresponding decrease in the amount of *trans* isomer (isomer nomenclature discussion in SI Section S4).

Compound 2 assembled in water (0.1 mg/mL) also shows a spectral change after 1 h of irradiation with UVA light similar to that observed in DMSO (Figure 3a). The photochemical

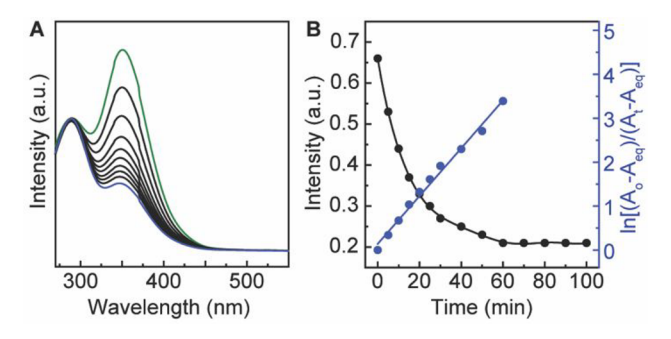


Figure 3. Nanoribbons from compound **2** in water show triggerable isomerization upon UVA irradiation. (a) Compound **2** exhibits a 67% drop in peak absorbance after 1 h of irradiation. The initial state is shown in green, and the photostationary state is shown in blue. (b) Time-dependent absorbance changes upon UVA irradiation of compound **2** are used to create a first-order plot of the *trans* to *cis* isomerization and extract a photoisomerization rate constant of $K = 5.44 \times 10^{-2}/\text{min}$.

reaction rate of 2 in water ($K = 5.44 \times 10^{-2}$ /min, Figure 3b) is slightly suppressed compared to its rate in DMSO ($K = 1.10 \times 10^{-1}$ /min). In addition, the reduction in peak absorbance intensity corresponding to the photoisomerization is decreased from 80% in DMSO to 67% in water. Changes in the state of soft matter driven by photochemical reactions are sensitive to their local environments, including polarity, viscosity, and light polarization, as well as the strength of intermolecular interactions when photochromic molecules are dissolved or dispersed in solvent.³⁵ Thus, we infer that the significant change in the molecules' local environments afforded by self-assembly impacts their measured photoisomerization kinetics.

We verify that nanostructures persist in water after photoisomerization by observing the Tyndall effect in solution. Compound 2 dissolved in DMSO before and after UVA exposure does not exhibit Tyndall scattering (i.e., light scattering upon red laser illumination indicative of the presence of nanostructures), and correspondingly no nanostructures are observed by AFM (Figure S22). Conversely, 2 in water displays significant Tyndall scattering before and after UVA irradiation, indicating the maintenance of nanostructures throughout the photoisomerization (Figure S22). AFM verifies the presence of nanoribbons before UVA irradiation and suggests a different nanotube structure afterward. We further demonstrate that the morphological transition of compound 2 in water is facilitated when the intensity of UVA light is increased (Figure S20).

With this information, we seek to understand the morphology of the *cis*-rich compound 2 assembly. We observe that compound 2 nanoribbons convert into nanotubes as the vinylnitrile moiety undergoes a *trans*-to-*cis* isomerization.

Initially, compound 2 nanoribbons mimic the structure of nanoribbons 1, as shown by TEM and SAXS (Figures 2e and 4a). The SAXS profile of an aqueous solution of 2 was best fit

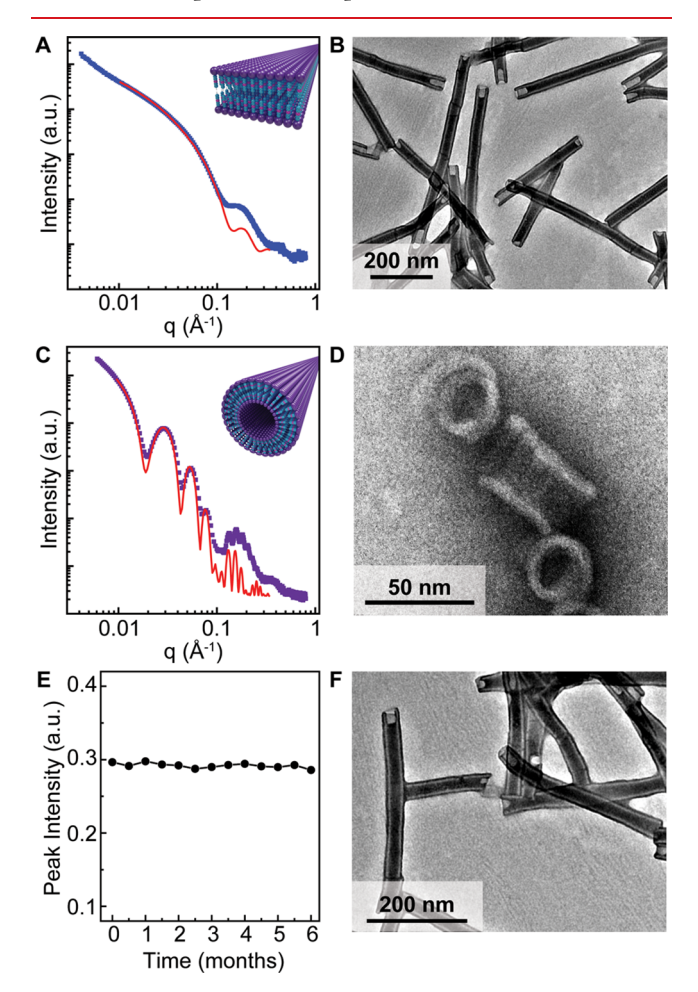


Figure 4. Compound 2 nanoribbons transition into nanotubes upon UVA irradiation and maintain their isomerized structure for at least six months. (a) Fitting of a rectangular prism model to SAXS of compound 2 nanoribbons is used to extract a 4.7 nm × 5.4 nm crosssection. (b) After 1 h of UVA irradiation, compound 2 nanoribbons convert into nanotubes observable by TEM. (c) Fitting of a hollow cylinder model to SAXS of compound 2 nanotubes reveals a 6.1 nm shell thickness and 19.4 nm core diameter. (d) Planar 2 nanoribbons coil under UVA light to form tight spirals in the nanoribbon to nanotube transition. The edges of the spirals fuse to form the observed final nanotube structure. (e) UV-vis absorption spectroscopy shows the maintenance of the same peak absorbance intensity corresponding to the cis state for six months, measured in half-month intervals. (f) Representative TEM of compound 2 nanotubes six months after UVA irradiation shows no evidence of nanoribbon formation.

to a rectangular prism model, returning nanoribbon dimensions of 4.7 nm in thickness and 5.4 nm in width (Figure S14).³⁷ Upon UVA irradiation of an aqueous solution of compound 2 nanoribbons for 1 h, the nanoribbons converted into nanotubes with a shell thickness comparable to the nanoribbon thickness (Figure 4b). The SAXS profile of the aqueous nanotube solution was fit to a hollow cylinder model with a 19.4 nm core diameter and a 6.1 nm shell thickness (Figure 4c, Figure S15).³⁸

The structural transition demonstrated in Figures 4a-c led us to investigate the mechanism of nanoribbon-to-nanotube morphological conversion in order to further understand the switching phenomena. We irradiated nanoribbons of 2 for just 10 min, rather than the typical irradiation time corresponding to the PSS, to capture its intermediate state. TEM of the solution at this time point shows an intermediate coiled ribbon nanostructure (Figure 4d). By comparing the dimensions of the nanoribbon coils to those of the nanotube itself, we can conclude that the photochemical reaction of amphiphiles within the nanoribbon assembly results in twisting of the nanoribbons to form tight coils, which then fuse to yield nanotubes. For context, folding of supramolecular nanoribbons into helical shapes without fusing, ^{39,40} toroid stacking to form tubular or helical structures, ⁴¹ and light-induced tubular disassembly ⁴² have been previously reported, but the mechanism shown here in the case of aramid amphiphiles has not previously been demonstrated as a response to photoisomerization in supramolecular assemblies. Similar mechanisms have been observed for chiral amphiphiles, bent core liquid crystals, and discotic polyaromatic hydrocarbons. 43-45

The formation of lamellar nanoribbons by the trans state of 2 is driven by dense intermolecular interactions between amphiphilic molecules. Compound 2 nanoribbons are constructed from layers of molecules aligned normal to the nanoribbon length axis. In the trans state, the molecules have a rod-like geometry, providing a feasible path for the formation of a nanoribbon morphology. Upon UVA irradiation for conversion of 2 to the cis state, the molecules take on a bentshape geometry and flexible conformation, resulting in local reorganization to compensate for space requirements. Diffraction on the subnanometer length scale provides local molecular packing information, so we perform 1D wide-angle X-ray diffraction (WAXD) on lyophilized samples of compound 2 nanostructures to elucidate this effect. 46 Weakening and broadening of sharp reflection peaks after UVA irradiation indicate that long-range molecular and shortrange positional orders are partially disrupted compared to the trans state (Figure S23). To maintain favorable interactions, we infer that the hydrophilic cationic head groups orient toward their aqueous environment, inducing curvature to the assembly. 47 Torsion induced by this curvature leads to the nanoribbon twisting, which ultimately fuses at the energetically unfavorable hydrophobic edges to produce nanotubes.

Reaching the PSS of **2** is similar to typical light-driven responses, but in contrast to that of previously reported materials, the isomerized product of **2** remains unchanged for several months after turning off UVA light (Figures 4e,f). The strongly interacting nature of compound **2** molecules in an assembled state, aided by hydrogen bonding and $\pi-\pi$ stacking in the aramid structural domain, drastically enhances their activation barrier for *cis*-to-*trans* isomerization, thereby increasing the nanotube lifetime. Consequently, we observe no nanotube-to-nanoribbon reversal at time points up to six months by UV—vis spectroscopy and TEM.

Finally, we investigated whether the isomerization reaction and consequent morphological transition are reversible by providing sufficient thermal energy for the vinylnitrile to revert to its *trans* ground state. Unable to overcome the activation barrier for reversibility at room temperature, we hypothesized that adding thermal energy could induce the reverse reaction as it increases the conformational dynamics within the nano-

structure, facilitating the one-bond-flip isomerization reaction from *cis* to *trans*. ^{49,50} Upon heating a solution of compound 2 nanoribbons to 80 °C for 1 h and cooling slowly, we observe a recovery in UV—vis absorbance to its original peak value. This heating and irradiation process can be repeated at least five times, indicating that the isomerization transition can be repeatedly performed on the nanostructures without loss (Figure 5a, Figure S21). The nanotube heating process fully regenerates nanoribbons with the same dimensions as their original assembled state (Figures 5b,c, Figure S16).

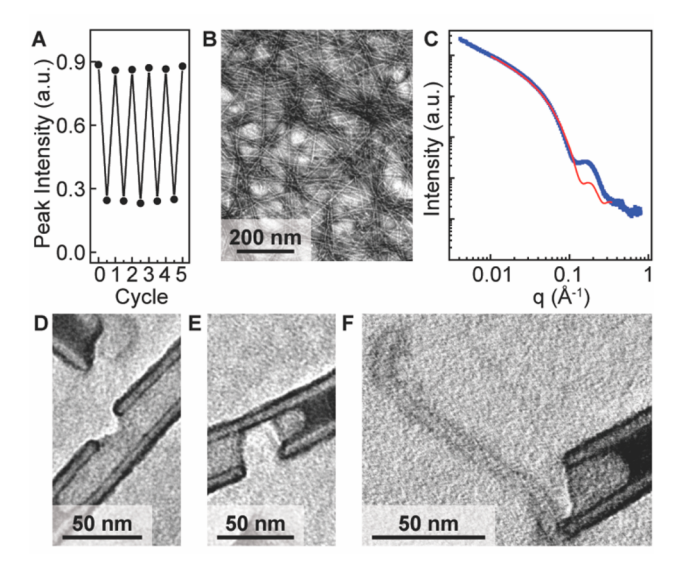


Figure 5. Photoisomerization of compound 2 from nanoribbons to nanotubes is reversed by heating at 80 °C for 1 h. (a) 2 isomerization is cyclically modulated over five cycles from repeated UVA irradiation and heating, as captured by tracking the peak absorbance intensity by UV—vis spectroscopy. (b) Representative TEM of compound 2 nanoribbons after 1 h of heating compound 2 nanotubes at 80 °C. (c) SAXS of compound 2 nanoribbons after heating from the nanotube morphology shows a return to its original dimensions, based on a rectangular prism fit (red). (d–f) Upon heating, compound 2 nanotubes rupture under torsional strain from isomerization, releasing nanoribbons that resemble the initial assemblies.

We again sought to capture the intermediate state of the morphological transition occurring with the reverse isomerization. The vinylnitrile *cis*-to-*trans* isomerization induces strain that causes rupture of the nanotube (Figure 5d). This rupture propagates across the nanotube to sciss the nanostructure (Figure 5e) and enables nanoribbon formation by unraveling of the nanotube at the interfaces (Figure 5f).

Here, we presented a photoresponsive aramid amphiphile (AA) platform for molecular self-assembly into supramolecular nanostructures. We demonstrate that the *trans*-to-*cis* photo-isomerization of constituent molecules triggers a morphological transition from nanoribbons to nanotubes. The nanotube state exhibits a long lifetime, especially for vinylnitrile moieties, of at least six months, achieved by employing the AA motif, a structure that exploits strong and extensive intermolecular interactions. We further demonstrated the reversibility of the morphological transition by providing sufficient thermal energy to induce the *cis*-to-*trans* conversion and recover the initial nanoribbon morphology. We captured the intermediate states of both morphological transitions to reveal their mechanisms: nanoribbon coiling and edge-to-edge

fusion to form nanotubes and nanotube fracture to release nanoribbons from the interfaces. This self-assembly platform could meet pressing challenges in responsive nanomaterial design by combining high nanostructure stability and long excited-state lifetimes with the capability to undergo phototriggered morphological transitions.

ASSOCIATED CONTENT

Supporting Information

The Supporting Information is available free of charge at https://pubs.acs.org/doi/10.1021/acs.nanolett.0c05048.

Materials, synthesis, sample preparation, isomer naming conventions, characterization details, SAXS fitting, statistical topographical analysis of nanoribbon contours, UV—vis controls and experiments, Tyndall effect, and proposed packing of 2 amphiphiles (PDF)

AUTHOR INFORMATION

Corresponding Author

Julia H. Ortony — Department of Materials Science and Engineering, Massachusetts Institute of Technology, Cambridge, Massachusetts 02139, United States; orcid.org/0000-0001-7446-6207; Email: ortony@mit.edu

Authors

Dae-Yoon Kim – Department of Materials Science and Engineering, Massachusetts Institute of Technology, Cambridge, Massachusetts 02139, United States; Institute of Advanced Composite Materials, Korea Institute of Science and Technology, Bondong, JB 55324, Korea

Ty Christoff-Tempesta – Department of Materials Science and Engineering, Massachusetts Institute of Technology, Cambridge, Massachusetts 02139, United States

Guillaume Lamour — LAMBE, Université Paris-Saclay, University of Evry, CNRS, Evry-Courcouronnes, France; orcid.org/0000-0002-9331-5532

Xiaobing Zuo — X-ray Science Division, Advanced Photon Source, Argonne National Laboratory, Argonne, Illinois 60439, United States

Ki-Hyun Ryu – Institute of Advanced Composite Materials, Korea Institute of Science and Technology, Bondong, JB 55324, Korea

Complete contact information is available at: https://pubs.acs.org/10.1021/acs.nanolett.0c05048

Author Contributions

¹D.-Y.K. and T.C.-T. contributed equally.

Funding

This material is based upon work supported by the National Science Foundation under Grant No. CHE-1945500. This work was supported in part by the Professor Amar G. Bose Research Grant Program and the Abdul Latif Jameel Water and Food Systems Lab. D.-Y.K. acknowledges the support of the Open Research Program (2E31332) of the Korea Institute of Science and Technology and the National Research Foundation of Korea (2021R1R1R1004226). T.C.-T. acknowledges the National Science Foundation Graduate Research Fellowship Program under Grant No. 1122374. G.L. acknowledges support from the University of Evry Paris-Saclay.

Note

The authors declare no competing financial interest.

ACKNOWLEDGMENTS

This work made use of the MRSEC Shared Experimental Facilities at MIT supported by the National Science Foundation under award number DMR-14-19807 and the MIT Department of Chemistry Instrumentation Facility (DCIF). X-ray scattering measurements were performed at beamline 12-ID-B of the Advanced Photon Source, a U.S. Department of Energy (DOE) Office of Science User Facility operated for the DOE Office of Science by Argonne National Laboratory under Contract No. DE-AC02-06CH11357.

ABBREVIATIONS

AA, aramid amphiphile; AFM, atomic force microscopy; DMSO, dimethyl sulfoxide; D₂O, deuterated water; DMSO-d, deuterated dimethyl sulfoxide; NMR, nuclear magnetic resonance; PSS, photostationary state; SAXS, small-angle X-ray scattering; TEM, transition electron microscopy; UV–vis, ultraviolet–visible

REFERENCES

- (1) Whitesides, G. M.; Mathias, J. P.; Seto, C. T. Molecular self-assembly and nanochemistry: a chemical strategy for the synthesis of nanostructures. *Science* **1991**, *254* (5036), 1312–1319.
- (2) Aida, T.; Meijer, E.; Stupp, S. I. Functional supramolecular polymers. *Science* **2012**, 335 (6070), 813–817.
- (3) Meng, Q.; Kou, Y.; Ma, X.; Liang, Y.; Guo, L.; Ni, C.; Liu, K. Tunable Self-Assembled Peptide Amphiphile Nanostructures. *Langmuir* **2012**, 28 (11), 5017–5022.
- (4) Cui, H.; Webber, M. J.; Stupp, S. I. Self-assembly of peptide amphiphiles: From molecules to nanostructures to biomaterials. *Biopolymers* **2010**, *94* (1), 1–18.
- (5) Fong, C.; Le, T.; Drummond, C. J. Lyotropic liquid crystal engineering-ordered nanostructured small molecule amphiphile self-assembly materials by design. *Chem. Soc. Rev.* **2012**, *41* (3), 1297–1322
- (6) Lis, L.; McAlister, d.; Fuller, N.; Rand, R.; Parsegian, V. Interactions between neutral phospholipid bilayer membranes. *Biophys. J.* **1982**, *37* (3), 657.
- (7) Rao, K. V.; George, S. J. Supramolecular Alternate Co-Assembly through a Non-Covalent Amphiphilic Design: Conducting Nanotubes with a Mixed D-A Structure. *Chem. Eur. J.* **2012**, *18* (45), 14286–14291.
- (8) Xu, Z.; Jia, S.; Wang, W.; Yuan, Z.; Ravoo, B. J.; Guo, D.-S. Heteromultivalent peptide recognition by co-assembly of cyclodextrin and calixarene amphiphiles enables inhibition of amyloid fibrillation. *Nat. Chem.* **2019**, *11* (1), 86–93.
- (9) Silva, G. A.; Czeisler, C.; Niece, K. L.; Beniash, E.; Harrington, D. A.; Kessler, J. A.; Stupp, S. I. Selective differentiation of neural progenitor cells by high-epitope density nanofibers. *Science* **2004**, *303* (5662), 1352–1355.
- (10) Ortony, J. H.; Newcomb, C. J.; Matson, J. B.; Palmer, L. C.; Doan, P. E.; Hoffman, B. M.; Stupp, S. I. Internal dynamics of a supramolecular nanofibre. *Nat. Mater.* **2014**, *13* (8), 812.
- (11) Nieh, M.-P.; Raghunathan, V. A.; Kline, S. R.; Harroun, T. A.; Huang, C.-Y.; Pencer, J.; Katsaras, J. Spontaneously formed unilamellar vesicles with path-dependent size distribution. *Langmuir* **2005**, 21 (15), 6656–6661.
- (12) Korevaar, P. A.; Newcomb, C. J.; Meijer, E. W.; Stupp, S. I. Pathway Selection in Peptide Amphiphile Assembly. *J. Am. Chem. Soc.* **2014**, *136* (24), 8540–8543.
- (13) Zhang, S. Fabrication of novel biomaterials through molecular self-assembly. *Nat. Biotechnol.* **2003**, *21* (10), 1171.
- (14) Christoff-Tempesta, T.; Lew, A. J.; Ortony, J. H. Beyond covalent crosslinks: applications of supramolecular gels. *Gels* **2018**, *4* (2), 40.

- (15) Dong, R.; Zhou, Y.; Huang, X.; Zhu, X.; Lu, Y.; Shen, J. Functional supramolecular polymers for biomedical applications. *Adv. Mater.* **2015**, *27* (3), 498–526.
- (16) Sun, L.; Zheng, C.; Webster, T. J. Self-assembled peptide nanomaterials for biomedical applications: promises and pitfalls. *Int. J. Nanomed.* **2017**, *12*, 73.
- (17) Zelzer, M.; Ulijn, R. V. Next-generation peptide nanomaterials: molecular networks, interfaces and supramolecular functionality. *Chem. Soc. Rev.* **2010**, *39* (9), 3351–3357.
- (18) Sur, S.; Matson, J. B.; Webber, M. J.; Newcomb, C. J.; Stupp, S. I. Photodynamic control of bioactivity in a nanofiber matrix. *ACS Nano* **2012**, *6* (12), 10776–10785.
- (19) Urban, P.; Pritzl, S. D.; Ober, M. F.; Dirscherl, C. F.; Pernpeintner, C.; Konrad, D. B.; Frank, J. A.; Trauner, D.; Nickel, B.; Lohmueller, T. A Lipid Photoswitch Controls Fluidity in Supported Bilayer Membranes. *Langmuir* **2020**, *36* (10), 2629–2634.
- (20) Wu, Z.; Xue, R.; Xie, M.; Wang, X.; Liu, Z.; Drechsler, M.; Huang, J.; Yan, Y. Self-Assembly-Triggered Cis-to-Trans Conversion of Azobenzene Compounds. J. Phys. Chem. Lett. 2018, 9 (1), 163–169
- (21) Zha, R. H.; Vantomme, G.; Berrocal, J. A.; Gosens, R.; de Waal, B.; Meskers, S.; Meijer, E. W. Photoswitchable Nanomaterials Based on Hierarchically Organized Siloxane Oligomers. *Adv. Funct. Mater.* **2018**, 28 (1), 1703952.
- (22) Maity, C.; Hendriksen, W. E.; van Esch, J. H.; Eelkema, R. Spatial structuring of a supramolecular hydrogel by using a visible-light triggered catalyst. *Angew. Chem., Int. Ed.* **2015**, *54* (3), 998–1001
- (23) Kathan, M.; Hecht, S. Photoswitchable molecules as key ingredients to drive systems away from the global thermodynamic minimum. *Chem. Soc. Rev.* **2017**, *46* (18), 5536–5550.
- (24) Gegiou, D.; Muszkat, K.; Fischer, E. Temperature dependence of photoisomerization. V. Effect of substituents on the photoisomerization of stilbenes and azobenzenes. *J. Am. Chem. Soc.* **1968**, 90 (15), 3907–3918.
- (25) Dyck, R. H.; McClure, D. S. Ultraviolet spectra of stilbene, p-monohalogen stilbenes, and azobenzene and the trans to cis photoisomerization process. *J. Chem. Phys.* **1962**, *36* (9), 2326–2345.
- (26) Zhu, H.; Shangguan, L.; Xia, D.; Mondal, J. H.; Shi, B. Control on the photo-responsive assembly of a stilbene-containing amphiphile by using pillar [5] arene-based host-guest interactions. *Nanoscale* **2017**, *9* (26), 8913–8917.
- (27) Bléger, D.; Schwarz, J.; Brouwer, A. M.; Hecht, S. o-Fluoroazobenzenes as readily synthesized photoswitches offering nearly quantitative two-way isomerization with visible light. *J. Am. Chem. Soc.* **2012**, *134* (51), 20597–20600.
- (28) Yao, X.; Li, T.; Wang, J.; Ma, X.; Tian, H. Recent progress in photoswitchable supramolecular self-assembling systems. *Adv. Opt. Mater.* **2016**, *4* (9), 1322–1349.
- (29) Choi, S.; Park, S. H.; Ziganshina, A. Y.; Ko, Y. H.; Lee, J. W.; Kim, K. A stable cis-stilbene derivative encapsulated in cucurbit [7] uril. *Chem. Commun.* **2003**, No. 17, 2176–2177.
- (30) Christoff-Tempesta, T.; Cho, Y.; Kim, D.-Y.; Geri, M.; Lamour, G.; Lew, A. J.; Zuo, X.; Lindemann, W. R.; Ortony, J. H. Self-assembly of aramid amphiphiles into ultra-stable nanoribbons and aligned nanoribbon threads. *Nat. Nanotechnol.* **2021**, DOI: 10.1038/s41565-020-00840-w.
- (31) Nallet, F.; Laversanne, R.; Roux, D. Modelling X-ray or neutron scattering spectra of lyotropic lamellar phases: interplay between form and structure factors. *J. Phys. II* 1993, 3 (4), 487–502.
- (32) Knowles, T. P.; Fitzpatrick, A. W.; Meehan, S.; Mott, H. R.; Vendruscolo, M.; Dobson, C. M.; Welland, M. E. Role of intermolecular forces in defining material properties of protein nanofibrils. *Science* **2007**, *318* (5858), 1900–1903.
- (33) Nassar, R.; Wong, E.; Gsponer, J. r.; Lamour, G. Inverse correlation between amyloid stiffness and size. *J. Am. Chem. Soc.* **2019**, 141 (1), 58–61.
- (34) Lamour, G.; Kirkegaard, J. B.; Li, H.; Knowles, T. P.; Gsponer, J. Easyworm: an open-source software tool to determine the

- mechanical properties of worm-like chains. Source code for biology and medicine 2014, 9 (1), 1-6.
- (35) Uchida, E.; Sakaki, K.; Nakamura, Y.; Azumi, R.; Hirai, Y.; Akiyama, H.; Yoshida, M.; Norikane, Y. Control of the orientation and photoinduced phase transitions of macrocyclic azobenzene. *Chem. Eur. J.* **2013**, *19* (51), 17391–17397.
- (36) Levchuk, I.; Hou, Y.; Gruber, M.; Brandl, M.; Herre, P.; Tang, X.; Hoegl, F.; Batentschuk, M.; Osvet, A.; Hock, R.; et al. Deciphering the role of impurities in methylammonium iodide and their impact on the performance of perovskite solar cells. *Adv. Mater. Interfaces* **2016**, 3 (22), 1600593.
- (37) Nayuk, R.; Huber, K. Formfactors of Hollow and Massive Rectangular Parallelepipeds at Variable Degree of Anisometry. *Z. Phys. Chem.* **2012**, 226 (7–8), 837–854.
- (38) Feigin, L.; Svergun, D. I. Structure analysis by small-angle X-ray and neutron scattering; Springer: 1987; Vol. 1.
- (39) Adhikari, B.; Yamada, Y.; Yamauchi, M.; Wakita, K.; Lin, X.; Aratsu, K.; Ohba, T.; Karatsu, T.; Hollamby, M. J.; Shimizu, N.; Takagi, H.; Haruki, R.; Adachi, S.-i.; Yagai, S. Light-induced unfolding and refolding of supramolecular polymer nanofibres. *Nat. Commun.* 2017, 8 (1), 15254.
- (40) Prabhu, D. D.; Aratsu, K.; Kitamoto, Y.; Ouchi, H.; Ohba, T.; Hollamby, M. J.; Shimizu, N.; Takagi, H.; Haruki, R.; Adachi, S.-i.; Yagai, S. Self-folding of supramolecular polymers into bioinspired topology. *Science Advances* **2018**, *4* (9), No. eaat8466.
- (41) Wang, H.; Lee, M. Switching between Stacked Toroids and Helical Supramolecular Polymers in Aqueous Nanotubules. *Macromol. Rapid Commun.* **2020**, *41* (11), 2000138.
- (42) Fredy, J. W.; Méndez-Ardoy, A.; Kwangmettatam, S.; Bochicchio, D.; Matt, B.; Stuart, M. C. A.; Huskens, J.; Katsonis, N.; Pavan, G. M.; Kudernac, T. Molecular photoswitches mediating the strain-driven disassembly of supramolecular tubules. *Proc. Natl. Acad. Sci. U. S. A.* 2017, 114 (45), 11850–11855.
- (43) Ziserman, L.; Lee, H.-Y.; Raghavan, S. R.; Mor, A.; Danino, D. Unraveling the mechanism of nanotube formation by chiral self-assembly of amphiphiles. *J. Am. Chem. Soc.* **2011**, *133* (8), 2511–2517
- (44) Wu, D.; Zhi, L.; Bodwell, G. J.; Cui, G.; Tsao, N.; Müllen, K. Self-assembly of positively charged discotic PAHs: from nanofibers to nanotubes. *Angew. Chem., Int. Ed.* **2007**, *46* (28), 5417–5420.
- (45) Kim, D.-Y.; Yoon, W.-J.; Choi, Y.-J.; Lim, S.-I.; Koo, J.; Jeong, K.-U. Photoresponsive chiral molecular crystal for light-directing nanostructures. *J. Mater. Chem. C* **2018**, *6* (45), 12314–12320.
- (46) Choi, Y.-J.; Jung, D.; Lim, S.-I.; Yoon, W.-J.; Kim, D.-Y.; Jeong, K.-U. Diacetylene-Functionalized Dendrons: Self-Assembled and Photopolymerized Three-Dimensional Networks for Advanced Self-Healing and Wringing Soft Materials. *ACS Appl. Mater. Interfaces* **2020**, *12* (29), 33239–33245.
- (47) Shadpour, S.; Nemati, A.; Boyd, N. J.; Li, L.; Prévôt, M. E.; Wakerlin, S. L.; Vanegas, J. P.; Salamończyk, M.; Hegmann, E.; Zhu, C.; et al. Heliconical-layered nanocylinders (HLNCs)-hierarchical self-assembly in a unique B4 phase liquid crystal morphology. *Mater. Horiz.* **2019**, *6* (5), 959–968.
- (48) Cano, M.; Sánchez-Ferrer, A.; Serrano, J. L.; Gimeno, N.; Ros, M. B. Supramolecular Architectures from Bent-Core Dendritic Molecules. *Angew. Chem.* **2014**, *126* (49), 13667–13671.
- (49) Zhu, L.; Li, X.; Zhang, Q.; Ma, X.; Li, M.; Zhang, H.; Luo, Z.; Ågren, H.; Zhao, Y. Unimolecular photoconversion of multicolor luminescence on hierarchical self-assemblies. *J. Am. Chem. Soc.* **2013**, 135 (13), 5175–5182.
- (50) Chung, J. W.; Yoon, S.-J.; An, B.-K.; Park, S. Y. High-contrast on/off fluorescence switching via reversible E-Z isomerization of diphenylstilbene containing the α -cyanostilbenic moiety. *J. Phys. Chem. C* **2013**, *117* (21), 11285–11291.